HHS Public Access

Author manuscript

Neurobiol Dis. Author manuscript; available in PMC 2025 May 28.

Published in final edited form as:

Neurobiol Dis. 2025 May ; 208: 106882. doi:10.1016/j.nbd.2025.106882.

Small molecule ion channel agonist/antagonist screen reveals seizure suppression *via* glial Irk2 activation in a Drosophila model of Dup15q syndrome

Benjamin Geier[a,b], **Bidisha Roy**[c], **Lawrence T. Reiter**[a,*]

[a]Department of Physiology, Tulane University, New Orleans, LA, USA

[b]Graduate Program in Neuroscience, Tulane University, New Orleans, LA, USA

[c]Department of Neurology, University of Tennessee Health Science Center, Memphis, TN, USA

Abstract

The neurogenetic disorder duplication 15q syndrome (Dup15q) is characterized by a high incidence of autism spectrum disorder (ASD) and pharmacoresistant epilepsy. Standard-of-care broad-spectrum anti-seizure medications (ASM) often fail to control seizures in Dup15q, emphasizing the need for the identification of new therapeutic compounds. Previously, we generated a model of Dup15q in *Drosophila melanogaster* by overexpressing *Dube3a* in glial cells, instead of neurons. This model recapitulates the spontaneous seizures present in Dup15q patients. Here, we screened a set of FDA-approved compounds for their ability to suppress seizures in *repo* > *Dube3a* flies. We used 72 compounds from the Enzo SCREEN-WELL Ion Channel Library for primary screening of seizure suppression. Six compounds were identified that significantly reduced seizure duration. Furthermore, the compounds that passed the primary and secondary screenings were associated with K^+ channels. Glial-specific knockdown of the inward rectifying potassium (*Irk*) 2 channel exacerbated the seizure phenotype in these animals indicating a mechanism of action for drugs that bind irk2, like minoxidil, and can suppress seizures through the rebalancing of K^+ extracellularly. This pharmacological and molecular investigation further supports the role of extracellular K^+ content in Dup15q seizure activation and provides a putative target for therapeutic intervention.

Keywords

Drosophila; Dup15q syndrome; Epilepsy; Drug screen; Ion channels

*Corresponding author. 1430 Tulane Ave., Hutchinson 4520A, New Orleans, LA 70112, USA, lreiter@tulane.edu (L.T. Reiter).

CRediT authorship contribution statement

Benjamin Geier: Writing – review & editing, Writing – original draft, Visualization, Methodology, Investigation, Formal analysis, Data curation, Conceptualization. **Bidisha Roy:** Writing – review & editing, Methodology, Investigation, Formal analysis, Data curation, Conceptualization. **Lawrence T. Reiter:** Validation, Supervision, Resources, Project administration, Methodology, Investigation, Funding acquisition, Conceptualization.

Declaration of competing interest

The authors declare no conflicts of interest.

Supplementary data to this article can be found online at https://doi.org/10.1016/j.nbd.2025.106882.

1. Introduction

Duplications and deletions at the 15q11.2-q13.1 locus are known to result in developmental disorders, including Prader-Willi syndrome (PWS), Angelman syndrome (AS), and Duplication 15q syndrome (Dup15q). This locus, also known as the Prader-Willi/Angelman syndrome critical region (PWACR), is genetically imprinted in mammals (Lusk et al., 1993). Dup15q syndrome results from duplications of the maternal PWACR, while AS and PWS are typically the result of a deletion in this same region (Hogart et al., 2010). The majority of Dup15q syndrome patients have two distinct forms of duplication: 1) interstitial duplication, which results in one additional copy of the 15q11.2-q13.1 locus within the maternal chromosome, or 2) isodicentric chromosome 15 (idic (15)), which results in the generation of a supernumerary chromosome with two copies of the locus ligated in an end-to-end fashion. Notably, idic(15) cases make up ~80 % of all Dup15q cases, and has a more severe clinical presentation (Lusk et al., 1993).

Children with Dup15q syndrome often experience high rates of autism spectrum disorder (ASD), developmental delays, gastrointestinal (GI) dysfunction, behavioral issues, and pharmacoresistant epilepsy. In idic (15) patients, over 65 % of individuals experience pharmacoresistant epilepsy (Lusk et al., 1993; Battaglia, 2008). Furthermore, of those who experience epilepsy, 81 % experience multiple seizure types (Conant et al., 2014). Broad-spectrum anti-seizure medications (ASM) commonly used to treat seizures prove efficacious in the short term; however, children with idic (15) will often be placed on two (sometimes three) ASMs over time because they stop working. Most parents with children who have idic (15) report these seizures to be the most problematic symptom of the disease (Conant et al., 2014).

Fortunately, only one gene is paternally imprinted in the 15q11.2-q13.1 locus. This gene, *UBE3A,* encodes for an E3 ligase known as ubiquitin-protein ligase E3A (UBE3A). This protein plays a crucial role in the ubiquitin-proteasome system (UPS), monoubiquitinating substrate proteins for the subsequent polyubiquitin chain that marks them for degradation *via* the proteasome (Finley, 2009; Zheng and Shabek, 2017). Imprinted expression of *UBE3A*, maternal allele specific, occurs in neurons (LaSalle et al., 2015). However, studies in mice with increased *Ube3a* expression in neurons fail to recapitulate the spontaneous seizures displayed in humans (Copping et al., 2017). This suggests that while neurons undergo genetic imprinting, they may not be the sole cell type involved in Dup15q pathogenesis.

Alternatively, *UBE3A* is not imprinted in glia in mice, monkeys and humans (Yamasaki et al., 2003; Dindot et al., 2008; Judson et al., 2014; Grier et al., 2015), and therefore expressed from both alleles in glial cells. Prior studies using cultured *Ube3a* neurons and glia showed the presence of the paternal antisense transcript (ATS) in neurons but not in glia (Yamasaki et al., 2003). Brain imaging studies using $Ube3a^{M-/P+}$ mice show no Ube3a signal in $NeuN^+$ neurons but do show detection of Ube3a in $GFAP^+$ glia (Judson et al., 2014). Recently, a study using rhesus macaque brains confirmed the presence of *UBE3A* in $SOX9^+$ glia, further supporting the bi-allelic glial expression of *UBE3A* (Gonzalez Ramirez et al., 2024). Furthermore, analysis of adult cerebral cortex samples demonstrated UBE3A expression in both $Olig2^+$ and $GFAP^+$ glial cells, conclusively confirming its presence in

glia (Burette et al., 2018). In cases of interstitial Dup15q syndrome, there are three active copies of *UBE3A* in glia, and in idic (15), this number may reach four functional copies in glial cells. Prior work in our lab using the model organism *Drosophila melanogaster* showed that when the Drosophila *UBE3A* ortholog, *Dube3a*, is elevated in glia, flies display seizures, paralleling patients with idic(15) (Hope et al., 2017). Additionally, these flies will experience spontaneous seizures with overexpression of either *Dube3a* or human *UBE3A*, suggesting a conserved mechanism from flies to humans (Landaverde et al., 2024).

In a previous study, we identified eight small molecules from the Prestwick Compound Library of previously approved compounds that significantly reduced seizure duration in our Dup15q fly seizure model (Roy et al., 2020). Here, we screened additional FDA-approved compounds from an ion channel-specific library (the Enzo Screen Well Ion Channel Library) to identify efficacious drugs for treating seizures in Dup15q patients. We also used drugs that passed primary and secondary screening to pinpoint a possible mechanism for why activation of certain K^+ ion channels suppresses seizures in the Dup15q fly model.

2. Results

2.1. Ion channel compound library screen reveals seizure suppression through the activation of K^+ channels

For primary screening of seizure suppressing compounds in *repo > Dube3a* flies we take advantage of a 30-s window of paralysis as previously described (Roy et al., 2020). After vortexing the flies, non-seizing flies are separated from seizing flies by letting them crawl up into a new vial (Roy et al., 2020), while paralyzed flies remain on the bottom. The Enzo SCREEN-WELL Ion Channel Library is comprised of a variety of ion channel agonists and antagonists. The library's composition consists of 37 % Ca^{2+}, 33 % K^+ agonists, and 30 % Na^+, Cl^- or Ca^{+2} inverse agonists (Fig. 1A). To pass the primary screen, >25 % of flies of the *repo > Dube3a* genotype (*w*^{1118};UAS-*Dube3a*;*repo*-GAL4) must actively climb the sorting apparatus for any given drug. Using this threshold, we identified 11 candidate suppressor compounds (Table 1). After completing the primary screen, we found that 55 % of the hit compounds were K^+ channel suppressors, suggesting a potential mechanism (Fig. 1B).

The 11 compound hits from the primary screen were tested at four different concentrations in a more rigorous secondary screen using the bang-sensitivity assay (BSA) (Benzer, 1971; Stone et al., 2014). During the BSA, flies are again vortexed to induce seizures and recovery times are recorded. Flies are grown on four different drug concentrations for each primary screen hit compound: 0.04 μM, 0.2 μM, 1 μM, and 5 μM. This allows for the identification of the lowest effective concentration that suppresses seizure activity in *repo > Dube3a* flies. To pass the secondary screen, the compound must reduce the seizure recovery time significantly and by at least 50 % in males and females compared to their respective solvent control (DMSO or EtOH). At least one drug concentration must reach a statistical significance of $p_{value} \leq 0.01$ compared to control flies.

In the secondary screen, we identified six compounds that significantly reduced seizure duration (Fig. 2). The drugs that did not pass the secondary screen can be found in Fig. S1.

Three of the six compounds that passed secondary screening work by targeting K^+ channels. These compounds include minoxidil, tolazamide, and NS-1619. The other three compounds that passed include Ryanodine, which activates Ca^{2+} channels; nitrendipine, which blocks Ca^{2+} channels; and quinidine, which blocks Na^+ channels.

2.2. In silico scRNA-seq analysis of Drosophila glia confirms Irk2 expression predominantly in astrocytes

Since three compounds that passed primary and secondary screening target K^+ channels, and based on our previous work showing that defects in glial regulation of K^+ homeostasis contribute to seizures in this model (Hope et al., 2017), we investigated the hypothesis that changes in extracellular K^+ levels affect seizure severity. One drug that passed the secondary screen, minoxidil, works as an inward rectifying potassium (Irk) channel agonist. Known as K_{ir} channels in mammals, Irk channels are crucial for maintaining homeostatic ion concentrations in neurons and are vital for glial resting membrane potential regulation (Hibino et al., 2010). To investigate this mechanism, we conducted knockdown (KD) experiments targeting Irk channels to determine their impact on seizure duration (Hibino et al., 2010). There are three Irk channels in the Drosophila genome: *Irk1*, *Irk2*, and *Irk3* (Dahal et al., 2017). In order to determine which channels are expressed in Drosophila astrocytes and thus would be able to regulate K^+ in glial cells, we performed *in silico* single cell expression studies to establish the appropriate *Irk* to use for knockdown studies. This step is crucial to understanding the mechanism of seizures in this model because astrocytes play a vital role in maintaining neuronal synapse homeostasis by regulating neurotransmitter reuptake, releasing neuroactive factors, and, most importantly, buffering ions (Walz, 2000; Perea and Araque, 2005; Sofroniew and Vinters, 2010).

Using the publicly available single-cell RNA-seq (scRNA-seq) database SCope (scope.aertslab.org) (Davie et al., 2018, Li, Janssens et al. Li et al., 2022), we analyzed single cell brain expression data by selecting both pan-glial (*repo*) and neuronal (*nSyb*) markers. T-distributed stochastic neighbor embedding (t-SNE) visualization revealed strong *Irk2* expression in the brain, with notably higher levels in cells identified as glia compared to neurons (Fig. S2). These findings align with previous studies identifying *Irk2* as the predominant isoform in the Drosophila brain (Luan and Li, 2012). To further characterize glial *Irk2* expression, we queried the glia scRNA-seq dataset specifically for *repo*-positive cells. The resulting t-SNE visualization showed robust *repo* expression across all clusters, confirming their identity as glia (Fig. S3). Next, we categorized these clusters using markers for distinct glial subtypes: *alrm* (astrocytes) and *moody* (subperineurial glia) (Stork et al., 2012). Given the crucial role of glia in ion homeostasis, we examined the co-expression of *Irk1*, *Irk2*, and *Irk3* within the *alrm*-positive cluster. Notably, *Irk2* expression was significantly enriched in astrocytes (Fig. 3), identifying *Irk2* as the predominant inward rectifier potassium channel in Drosophila astrocytes.

2.3. Glial knockdown of Irk2 channels exacerbates seizure phenotypes in repo > Dube3a flies

K^+ channel activation significantly reduces seizure duration in *repo* > *Dube3a* flies, highlighting the role of K^+ channels in modulating neuronal excitability in this seizure

model. Since minoxidil specifically targets Irk channels, we investigated the effect of *Irk2* knockdown (KD) on seizure susceptibility. To test this, we expressed an RNAi for *Irk2* in the context of glial overexpression of *Dube3a*. We crossed w^{1118}; [*repo*-GAL4;UAS-*Dube3a*]/X(2:3)*ap* flies with a UAS-*Irk2-RNAi* line, thereby overexpressing *Dube3a* in all glial cells while simultaneously knocking down *Irk2*. Consistent with previous observations, treatment with 0.04 μM minoxidil, a known K^+ channel activator, significantly reduced seizure duration in *repo* > *Dube3a* flies compared to those treated with the vehicle control. However, in *repo* > *Dube3a/Irk2*-RNAi flies, the knockdown of *Irk2* nullified the therapeutic effect of minoxidil when compared to *repo* > *Dube3a* flies alone (Fig. 4). These results emphasize the importance of glial Irk2 channels in the regulation of K^+ clearance during intensified neuronal excitability. By removing the target of minoxidil (Irk2), the drug is no longer able to suppress seizure behavior. These results implicate glial Irk2 channels in the mechanism of seizure suppression by minoxidil.

2.4. Minoxidil treatment rescues intracellular glial K^+ content in repo > *Dube3a flies*

Since minoxidil is an Irk2 agonist that suppresses seizure activity in our *repo* > *Dube3a* model we looked for changes in glial K^+ content as a possible mechanism. Previously we showed that *repo* > *Dube3a* flies have significantly reduced intracellular K^+ concentration ($[K^+]_i$) compared to control flies (Hope et al., 2017; Roy et al., 2020). We used ION Potassium Green – 2 (IPG-2), a known potassium sensing dye, in unfixed adult brains to assess changes in glial $[K^+]_i$ levels (Rana et al., 2019). We dissected brains from three-day-old *repo* > *tdTomato* or *repo* > *Dube3a*; *tdTomato* flies treated with either EtOH or 0.04 μM minoxidil. We then quantified IPG-2 signal in tdTomato positive glia to assess whether the addition of minoxidil promoted K^+ uptake. As in our previous seizure suppression study, we saw a significant $[K^+]_i$ reduction in *repo* > *Dube3a; tdTomato* flies compared to their *repo* > *tdTomato* counterparts (Fig. 5A *vs* 5B). However, *repo* > *Dube3a; tdTomato* flies treated with minoxidil showed complete rescue of $[K^+]_i$ levels (Fig. 5C). Not only does this data provide further support for the pharmacological mechanism of minoxidil but also expands on the crucial role of K^+ clearance in suppressing gliopathic epilepsy in our model.

3. Discussion

In this study, we applied a proven Drosophila Dup15q syndrome drug screening approach to identify additional candidate therapeutic compounds that can suppress seizures in our fly model of Dup15q epilepsy. Using the Enzo SCREEN-WELL Ion Channel Ligand Library, we identified six compounds that significantly reduce seizure duration in *repo* > *Dube3a* flies. In addition, half of the compounds that passed the secondary screening act on K^+ channels. *In silico* analysis of the Drosophila glial scRNA-seq dataset (scope.aertslab.org) determined that *Irk2* is almost exclusively expressed in glia, with strong expression in astrocytes. We found that glial-specific knockdown of *Irk2* exacerbates the seizure phenotype in *repo* > *Dube3a; Irk2-RNAi* flies even when treated with the K^+ channel activator minoxidil supporting our hypothesis that normalizing K^+ homeostasis is critical to rescue of the seizure phenotype. Furthermore, using the K^+ sensing dye IPG-2, we demonstrated a rescue of $[K+]_i$ in *repo* > *Dube3a; tdTomato* flies, highlighting not only

the mechanism of action for minoxidil but also the critical role of K^+ balance in gliopathic epilepsy.

There is a significant role for glia in ion buffering, linking K^+ buffering to epileptogenic events (Schröder et al., 2000; Clapcote et al., 2009; Haj-Yasein et al., 2011; Heuser et al., 2012; Du et al., 2018). Neuronal activity induces transient increases in extracellular K^+ concentration ($[K^+]_o$). In conjunction, rises in $[K^+]_o$ have been shown to increase neuronal excitability (Scharfman, 2007; Seifert and Steinhäuser, 2013; Larsen et al., 2016). These findings emphasize a critical role for astrocytes in maintaining proper ion balance within the brain. To manage $[K^+]_o$, astrocytes have been shown to use $Na^+/K^+/Cl^-$ cotransporters, Na^+/K^+ pumps, and K_{ir} channels (Cholet et al., 2002; Bellot-Saez et al., 2017; Walch et al., 2020). Previously, our lab showed that overexpression of *Dube3a* in glia significantly reduces a Na^+/K^+ ATPα ion channel. Using a K^+ sensing dye, we showed a significant decrease in glial K^+ content for *repo > Dube3a; tdTomato* flies compared to *repo > +; tdTomato* control, suggesting ion buffering deficits. Furthermore, we showed that reintroducing ATPα to *Dube3a* overexpressing flies significantly reduced the seizure duration, indicating a critical role in seizure pathogenesis, while the Na^+/K^+ inhibitor ouabain had the opposite effect (Hope et al., 2017). Our findings here suggest that the activation of Irk2 channels significantly reduces seizure duration in *repo > Dube3a* flies, which aligns with the previous work indicating a role for K^+ levels in seizure susceptibility. Pharmacologically activating Irk2 channels in astrocytes with minoxidil helps reduce neuronal excitability by reducing $[K^+]_o$ (Fig. 6).

The other two drugs that act on K^+ channels, tolazamide and NS-1619, also showed significant reductions in seizure duration, but one is an inhibitor of Kir channels. Tolazamide, a sulfonylurea commonly used to treat type 2 diabetes, targets sulfonylurea receptors (SURs) on Kir channels in pancreatic beta cells, stimulating insulin release and lowering blood sugar levels (Graal and Wolffenbuttel, 1999; Harrigan et al., 2001). Interestingly, while inhibition of Kir channels by tolazamide might initially seem counterintuitive in the context of seizure reduction, closer examination reveals a plausible mechanism. In fruit flies, insulin-producing cells (IPCs) secrete insulin-like peptides (ILPs) that regulate glucose homeostasis (Fernandez et al., 1995; Brogiolo et al., 2001; Rulifson et al., 2002). Tolazamide's activation of IPCs likely induces a net decrease in glucose, which aligns with evidence linking stabilized glucose levels to decreased seizure intensity (McILwAIN, 1969; Schwechter et al., 2003; Stafstrom, 2003; Schauwecker, 2012). Given the fruit fly diet is high in sugar, the observed reduction in seizure duration with tolazamide may result from its ability to reduce glucose levels, mitigating seizure severity.

NS-1619 selectively activates large-conductance calcium-activated potassium (BK) channels, which are abundantly expressed in neurons and play critical roles in neurotransmitter release, muscle contraction, and auditory function (Contet et al., 2016; Pyott and Duncan, 2016). BK channel activation hyperpolarizes the cell membrane by facilitating potassium efflux, reducing neuronal excitability. Because of their extensive expression throughout the human brain, the activation of BK channels by NS-1619 likely induces global hyperpolarization. This raises the threshold for depolarization, thereby

decreasing the likelihood of unwanted action potentials in an already hyperexcitable brain and suppressing epileptiform activity.

While much of our work focused on unraveling the mechanistic role of K^+ buffering on seizure susceptibility, we found three other compounds in the screen that had different mechanisms of action (MoA). Ryanodine, a Ca^{2+} channel agonist, binds ryanodine receptors (RyRs), releasing Ca^{2+} from the sarcoplasmic reticulum generating muscle contractions. However, at higher concentrations, ryanodine can lead to paralysis and even death in both mammals and insects (Marks, 2023). While the drug did pass secondary screening, it should be noted that it only passed at our lowest concentration, 0.04 μM. Moreover, concentrations above 0.2 μM became lethal, aligning with previous studies. Another drug, nitrendipine, is an L-type Ca^{2+} channel (LTCC) blocker used to treat hypertension. LTCCs are highly prevalent in neurons and muscle cells. It has been shown that LTCCs play a crucial role in modulating intracellular Ca^{2+} concentrations ($[Ca^{2+}]_i$) during a neuron's basal state and subthreshold depolarization (Lee, Lee et al., 2023). The regulation of $[Ca^{2+}]_i$ is critical for intracellular signaling cascades that promote neurotransmitter release (Junge et al., 2004; Lipstein et al., 2013). By pharmacologically blocking LTCCs, one can presume that this impedes the brain's net neurotransmission. Thus, the significant reduction in seizure activity seen in *repo > Dube3a* flies treated with nitrendipine may be attributed to reductions in global neuronal excitability by blocking LTCCs. The final ion channel drug identified, quinidine, is a class I_A antiarrhythmic drug that non-selectively inhibits cardiac cation channels. Notably, in cases of *KCNT1*-related epilepsy, quinidine has been shown to have moderate success (Mikati et al., 2015; Liu et al., 2023; Gras et al., 2024). *KCNT1* encodes for a sodium-activated potassium channel ($K_{Na}1.1$). Gain-of-function $K_{Na}1.1$ variants increase hyperexcitability, explaining why treatment with a non-specific cation blocker like quinidine has shown moderate efficacy.

While our findings emphasize the role of K^+ buffering deficits in *Dube3a*-induced seizure susceptibility, the identification of compounds targeting non–K^+ channels suggest additional contributing mechanisms. The effectiveness of nitrendipine and quinidine implies that disruptions in Ca^{2+} and broader cation homeostasis may also play a role in seizure pathogenesis. Additionally, the seizure-suppressing effect of tolazamide suggests a potential metabolic component, as astrocytes regulate glucose availability for neuronal function (Staricha et al., 2020). Moreover, given the critical role of astrocytes in neurotransmitter clearance, *Dube3a* overexpression may impair glutamate uptake, leading to heightened seizure susceptibility (Mahmoud et al., 2019). Future studies will be needed to disentangle these mechanisms and determine their relative contributions to Dup15q-associated epilepsy.

In summary, here we identified six FDA-approved compounds that show potential for reducing seizure severity in individuals with pharmacoresistant Dup15q-associated epilepsy by specifically targeting ion channels in both glia and neurons. Furthermore, results from the screen combined with *Irk2* KD experiments highlight a potential link between astrocytic K^+ spatial buffering deficits, driven by Dube3a overexpression, and the development of pharmacoresistant epilepsy in Dup15q syndrome. Since human *UBE3A* is not imprinted in glial cells (Yamasaki et al., 2003), it is potentially elevated in astrocytes in the human brain,

making our model and this work directly translational in treating Dup15q pharmacoresistant epilepsy.

4. Methods and materials

4.1. Fly stocks and drug screening

Fly stocks were maintained on standard Drosophila corn meal media (Bloomington Stock Center) at 25 °C on a 12-h light/dark cycle. The following line was acquired from the Bloomington Drosophila Stock Center (BDSC): UAS-*Irk2*-RNAi (BDSC#, 58,333). All other lines used in these studies can be provided upon request.

4.2. Compound preparation

The SCREEN-WELL Ion Channel Ligand Library was acquired from Enzo Life Sciences. This library comprises 70 FDA-approved ion channel blockers and openers that are ideal candidates for our drug screening purposes. All compounds were dissolved in the appropriate solvent (DMSO or EtOH) and mixed with standard corn meal medium at a final working concentration of 1 μM. For the secondary screen, all compounds were dissolved and mixed with standard corn meal medium at working concentrations of 0.04 μM, 0.2 μM, 1 μM, and 5 μM.

4.3. Primary drug screen

The primary screen was essentially performed as in Roy et al., 2020 (Roy et al., 2020). Briefly, to avoid unanticipated behavioral issues during our screening, flies were not exposed to CO_2 for at least two days before testing. 3–5-day-old flies in both the drug and non-drug groups were transferred to empty vials and then subjected to 10 s of vortexing at maximum speed. Afterward, within a 30-s critical window, flies were separated (seizing *vs.* non-seizing) with the help of a previously described fly sorting apparatus (Roy et al., 2020). The apparatus used was comprised of a 50 mL falcon tube cut at both ends with a small funnel at the top and placed in a petri dish. Seizing flies are poured down the funnel into the cut falcon tube. Quickly, the funnel is replaced with a second tube, which exploits the innate negative geotaxis of the fruit fly and allows for separation. After 30 s, the petri dish containing the seizing flies and the tube containing the recovered flies are quickly capped. Flies within the petri dish (seizing) and the tube (recovered) are then counted for analysis. Both *repo > Dube3a* and UAS-*Dube3a; TM3, Sb* flies were counted during the primary screen. However, because only the *repo > Dube3a* flies experienced seizures, we only use these values to calculate the percent suppression.

4.4. Secondary drug screen

Secondary screening was also performed as in Roy et al., 2020 (Roy et al., 2020). For the secondary drug screen, flies were sorted by genotype and gender three days before testing to avoid CO2-related complications. Male and female *repo > Dube3a* flies were transferred to fresh food vials containing the corresponding drug of interest. Once flies mature to 3–5 days old, they are anesthetized by placing them on ice for 2–3 min. Flies are then distributed to empty fly vials for BSA analysis, with no more than five flies per vial. After at least one hour of recovery, flies are subjected to vortexing at max speed for 10 s. Each fly has its total

recovery time recorded. Total recovery is defined by the time it takes for the fly to stand up and move freely in the vial. For each compound, a minimum of 30 male and female animals are tested in the BSA to ensure statistical power.

4.5. Glial cell K^+ content assay

IPG-2 AM is a cell-permeable potassium (K^+) indicator. Three-day-old *repo > tdTomato* or *repo > Dube3a*; *tdTomato* flies were reared on food containing either EtOH (control) or 0.04 μM minoxidil. Flies were anesthetized, and their brains were dissected and stored in Drosophila saline solution. The Drosophila saline solution is comprised of the following (in mM): 128 NaCl, 1.8 CaCl, 2 KCl, $5MgCl_2$, 36 sucrose, 5 HEPES pH 7.2. The dissected brains were incubated for one hour in Drosophila saline containing 4.4 μM IPG-2. Following incubation, brains were washed twice in fresh Drosophila saline and wet-mounted in Drosophila saline on microscope slides. Optic lobes were imaged using an Olympus BX51 microscope with a 60× oil immersion lens and colour filters for tdTomato and IPG-2 fluorescence. For each condition, 20 tdTomato positive cells per optic lobe were analyzed across at least six flies. Each animal had all cells from each animal were averaged and normalized to the *repo > tdTomato* control condition.

4.6. Data analysis

All data analysis was performed using Prism 10 (GraphPad). The secondary BSA, the *Irk2* KD, and IPG-2 analysis was performed using one-way ANOVA with Dunnett's multiple comparison test. For all statistical tests, we set the α to 0.05. All graphs shown are mean ± SEM. p_{value} are as follows: *$p \leq .05$, ** $p \leq .01$, *** $p \leq .001$, **** $p \leq .0001$. All figures were generated using Adobe Illustrator (Adobe).

Supplementary Material

Refer to Web version on PubMed Central for supplementary material.

Acknowledgments

This work was supported by an NIH/NINDS grant to LTR (1R01NS115776-01A1). We acknowledge using stocks from Bloomington Drosophila Stock Center (P40OD018537), graphic design assistance from BioRender (Biorender.com) and open-access data from the SCope scRNA-seq database (scope.aertslab.org). We would also like to thank lab members and colleagues for their critical review of the manuscript.

Data availability

All data generated during this study are included in this manuscript and can also be found via download through Figshare (10.6084/m9.figshare.28236113).

References

Battaglia A, 2008. The inv dup (15) or idic (15) syndrome (Tetrasomy 15q). Orphanet J. Rare Dis 3, 30. [PubMed: 19019226]

Bellot-Saez A, Kékesi O, Morley JW, Buskila Y, 2017. Astrocytic modulation of neuronal excitability through K(+) spatial buffering. Neurosci. Biobehav. Rev 77, 87–97. [PubMed: 28279812]

Benzer S, 1971. From the gene to behavior. Jama 218 (7), 1015–1022. [PubMed: 4942064]

Brogiolo W, Stocker H, Ikeya T, Rintelen F, Fernandez R, Hafen E, 2001. An evolutionarily conserved function of the Drosophila insulin receptor and insulin-like peptides in growth control. Curr. Biol 11 (4), 213–221. [PubMed: 11250149]

Burette AC, Judson MC, Li AN, Chang EF, Seeley WW, Philpot BD, Weinberg RJ, 2018. Subcellular organization of UBE3A in human cerebral cortex. Mol. Autism 9, 54. [PubMed: 30364390]

Cholet N, Pellerin L, Magistretti PJ, Hamel E, 2002. Similar perisynaptic glial localization for the Na+,K+-ATPase alpha 2 subunit and the glutamate transporters GLAST and GLT-1 in the rat somatosensory cortex. Cereb. Cortex 12 (5), 515–525. [PubMed: 11950769]

Clapcote SJ, Duffy S, Xie G, Kirshenbaum G, Bechard AR, Rodacker Schack V, Petersen J, Sinai L, Saab BJ, Lerch JP, Minassian BA, Ackerley CA, Sled JG, Cortez MA, Henderson JT, Vilsen B, Roder JC, 2009. Mutation I810N in the alpha3 isoform of Na+,K+-ATPase causes impairments in the sodium pump and hyperexcitability in the CNS. Proc. Natl. Acad. Sci. USA 106 (33), 14085–14090. [PubMed: 19666602]

Conant KD, Finucane B, Cleary N, Martin A, Muss C, Delany M, Murphy EK, Rabe O, Luchsinger K, Spence SJ, Schanen C, Devinsky O, Cook EH, LaSalle J, Reiter LT, Thibert RL, 2014. A survey of seizures and current treatments in 15q duplication syndrome. Epilepsia 55 (3), 396–402. [PubMed: 24502430]

Contet C, Goulding SP, Kuljis DA, Barth AL, 2016. BK channels in the central nervous system. Int. Rev. Neurobiol 128, 281–342. [PubMed: 27238267]

Copping NA, Christian SGB, Ritter DJ, Islam MS, Buscher N, Zolkowska D, Pride MC, Berg EL, LaSalle JM, Ellegood J, Lerch JP, Reiter LT, Silverman JL, Dindot SV, 2017. Neuronal overexpression of Ube3a isoform 2 causes behavioral impairments and neuroanatomical pathology relevant to 15q11.2-q13.3 duplication syndrome. Hum. Mol. Genet 26 (20), 3995–4010. [PubMed: 29016856]

Dahal GR, Pradhan SJ, Bates EA, 2017. Inwardly rectifying potassium channels influence Drosophila wing morphogenesis by regulating Dpp release. Development 144 (15), 2771–2783. [PubMed: 28684627]

Davie K, Janssens J, Koldere D, De Waegeneer M, Pech U, Kreft Ł, Aibar S, Makhzami S, Christiaens V, Bravo González-Blas C, Poovathingal S, Hulselmans G, Spanier KI, Moerman T, Vanspauwen B, Geurs S, Voet T, Lammertyn J, Thienpont B, Liu S, Konstantinides N, Fiers M, Verstreken P, Aerts S, 2018. A single-cell transcriptome atlas of the aging Drosophila brain. Cell 174 (4), 982–998.e920. [PubMed: 29909982]

Dindot SV, Antalffy BA, Bhattacharjee MB, Beaudet AL, 2008. The Angelman syndrome ubiquitin ligase localizes to the synapse and nucleus, and maternal deficiency results in abnormal dendritic spine morphology. Hum. Mol. Genet 17 (1), 111–118. [PubMed: 17940072]

Du M, Li J, Chen L, Yu Y, Wu Y, 2018. Astrocytic Kir4.1 channels and gap junctions account for spontaneous epileptic seizure. PLoS Comput. Biol 14 (3), e1005877. [PubMed: 29590095]

Fernandez R, Tabarini D, Azpiazu N, Frasch M, Schlessinger J, 1995. The Drosophila insulin receptor homolog: a gene essential for embryonic development encodes two receptor isoforms with different signaling potential. EMBO J. 14 (14), 3373–3384. [PubMed: 7628438]

Finley D, 2009. Recognition and processing of ubiquitin-protein conjugates by the proteasome. Annu. Rev. Biochem 78, 477–513. [PubMed: 19489727]

Gonzalez Ramirez C, Salvador SG, Patel RKR, Clark S, Miller NW, James LM, Ringelberg NW, Simon JM, Bennett J, Amaral DG, Burette AC, Philpot BD, 2024. Regional and cellular organization of the autism-associated protein UBE3A/E6AP and its antisense transcript in the brain of the developing rhesus monkey. Front. Neuroanat 18, 1410791. [PubMed: 38873093]

Graal MB, Wolffenbuttel BH, 1999. The use of sulphonylureas in the elderly. Drugs Aging 15 (6), 471–481. [PubMed: 10641958]

Gras M, Bearden D, West J, Nabbout R, 2024. Efficacy of anti-seizure medications and alternative therapies (ketogenic diet, CBD, and quinidine) in KCNT1-related epilepsy: a systematic review. Epilepsia Open 9 (4), 1176–1191. [PubMed: 39093319]

Grier MD, Carson RP, Lagrange AH, 2015. Toward a broader view of Ube3a in a mouse model of Angelman syndrome: expression in brain, spinal cord, sciatic nerve and glial cells. PLoS One 10 (4), e0124649. [PubMed: 25894543]

Haj-Yasein NN, Jensen V, Vindedal GF, Gundersen GA, Klungland A, Ottersen OP, Hvalby O, Nagelhus EA, 2011. Evidence that compromised K+ spatial buffering contributes to the epileptogenic effect of mutations in the human Kir4.1 gene (KCNJ10). Glia 59 (11), 1635–1642. [PubMed: 21748805]

Harrigan RA, Nathan MS, Beattie P, 2001. Oral agents for the treatment of type 2 diabetes mellitus: pharmacology, toxicity, and treatment. Ann. Emerg. Med 38 (1), 68–78. [PubMed: 11423816]

Heuser K, Eid T, Lauritzen F, Thoren AE, Vindedal GF, Taubøll E, Gjerstad L, Spencer DD, Ottersen OP, Nagelhus EA, de Lanerolle NC, 2012. Loss of perivascular Kir4.1 potassium channels in the sclerotic hippocampus of patients with mesial temporal lobe epilepsy. J. Neuropathol. Exp. Neurol 71 (9), 814–825. [PubMed: 22878665]

Hibino H, Inanobe A, Furutani K, Murakami S, Findlay I, Kurachi Y, 2010. Inwardly rectifying potassium channels: their structure, function, and physiological roles. Physiol. Rev 90 (1), 291–366. [PubMed: 20086079]

Hogart A, Wu D, LaSalle JM, Schanen NC, 2010. The comorbidity of autism with the genomic disorders of chromosome 15q11.2-q13. Neurobiol. Dis 38 (2), 181–191. [PubMed: 18840528]

Hope KA, LeDoux MS, Reiter LT, 2017. Glial overexpression of Dube3a causes seizures and synaptic impairments in Drosophila concomitant with down regulation of the Na(+)/K(+) pump ATPα. Neurobiol. Dis 108, 238–248. [PubMed: 28888970]

Judson MC, Sosa-Pagan JO, Del Cid WA, Han JE, Philpot BD, 2014. Allelic specificity of Ube3a expression in the mouse brain during postnatal development. J. Comp. Neurol 522 (8), 1874–1896. [PubMed: 24254964]

Junge HJ, Rhee JS, Jahn O, Varoqueaux F, Spiess J, Waxham MN, Rosenmund C, Brose N, 2004. Calmodulin and Munc13 form a Ca2+ sensor/effector complex that controls short-term synaptic plasticity. Cell 118 (3), 389–401. [PubMed: 15294163]

Landaverde S, Sleep M, Lacoste A, Tan S, Schuback R, Reiter LT, Iyengar A, 2024. Glial expression of Drosophila UBE3A causes spontaneous seizures that can be modulated by 5-HT signaling. Neurobiol. Dis 200, 106651. [PubMed: 39197537]

Larsen BR, Stoica A, MacAulay N, 2016. Managing brain extracellular K(+) during neuronal activity: the physiological role of the Na(+)/K(+)-ATPase subunit isoforms. Front. Physiol 7, 141. [PubMed: 27148079]

LaSalle JM, Reiter LT, Chamberlain SJ, 2015. Epigenetic regulation of UBE3A and roles in human neurodevelopmental disorders. Epigenomics 7 (7), 1213–1228. [PubMed: 26585570]

Lee BJ, Lee U, Ryu SH, Han S, Lee SY, Lee JS, Ju A, Chang S, Lee SH, Kim SH, Ho WK, 2023. L-type ca(2+) channels mediate regulation of glutamate release by subthreshold potential changes. Proc. Natl. Acad. Sci. USA 120 (12), e2220649120.

Li H, Janssens J, De Waegeneer M, Kolluru SS, Davie K, Gardeux V, Saelens W, David FPA, Brbić M, Spanier K, Leskovec J, McLaughlin CN, Xie Q, Jones RC, Brueckner K, Shim J, Tattikota SG, Schnorrer F, Rust K, Nystul TG, Carvalho-Santos Z, Ribeiro C, Pal S, Mahadevaraju S, Przytycka TM, Allen AM, Goodwin SF, Berry CW, Fuller MT, White-Cooper H, Matunis EL, DiNardo S, Galenza A, O'Brien LE, Dow JAT, Jasper H, Oliver B, Perrimon N, Deplancke B, Quake SR, Luo L, Aerts S, Agarwal D, Ahmed-Braimah Y, Arbeitman M, Ariss MM, Augsburger J, Ayush K, Baker CC, Banisch T, Birker K, Bodmer R, Bolival B, Brantley SE, Brill JA, Brown NC, Buehner NA, Cai XT, Cardoso-Figueiredo R, Casares F, Chang A, Clandinin TR, Crasta S, Desplan C, Detweiler AM, Dhakan DB, Donà E, Engert S, Floc'hlay S, George N, González-Segarra AJ, Groves AK, Gumbin S, Guo Y, Harris DE, Heifetz Y, Holtz SL, Horns F, Hudry B, Hung RJ, Jan YN, Jaszczak JS, Jefferis G, Karkanias J, Karr TL, Katheder NS, Kezos J, Kim AA, Kim SK, Kockel L, Konstantinides N, Kornberg TB, Krause HM, Labott AT, Laturney M, Lehmann R, Leinwand S, Li J, Li JSS, Li K, Li K, Li L, Li T, Litovchenko M, Liu HH, Liu Y, Lu TC, Manning J, Mase A, Matera-Vatnick M, Matias NR, McDonough-Goldstein CE, McGeever A, McLachlan AD, Moreno-Roman P, Neff N, Neville M, Ngo S, Nielsen T, O'Brien CE, Osumi-Sutherland D, Özel MN, Papatheodorou I, Petkovic M, Pilgrim C, Pisco AO, Reisenman C, Sanders EN, Santos G Dos Scott K, Sherlekar A, Shiu P, Sims D, Sit RV, Slaidina M, Smith HE, Sterne G, Su YH, Sutton D, Tamayo M, Tan M, Tastekin I, Treiber C, Vacek D, Vogler G, Waddell S, Wang W, Wilson RI, Wolfner MF, Wong YE, Xie A, Xu J, Yamamoto S, Yan J, Yao Z, Yoda K, Zhu R,

Zinzen RP, 2022. Fly cell atlas: a single-nucleus transcriptomic atlas of the adult fruit fly. Science 375 (6584), eabk2432. [PubMed: 35239393]

Lipstein N, Sakaba T, Cooper BH, Lin KH, Strenzke N, Ashery U, Rhee JS, Taschenberger H, Neher E, Brose N, 2013. Dynamic control of synaptic vesicle replenishment and short-term plasticity by Ca(2+)-calmodulin-Munc13–1 signaling. Neuron 79 (1), 82–96. [PubMed: 23770256]

Liu R, Sun L, Wang Y, Wang Q, Wu J, 2023. New use for an old drug: quinidine in KCNT1-related epilepsy therapy. Neurol. Sci 44 (4), 1201–1206. [PubMed: 36437393]

Luan Z, Li HS, 2012. Inwardly rectifying potassium channels in Drosophila. Sheng Li Xue Bao 64 (5), 515–519. [PubMed: 23090492]

Lusk L, Vogel-Farley V, DiStefano C, Jeste S, 1993. In: Adam MP, Feldman J, Mirzaa GM, et al. (Eds.), Maternal 15q Duplication Syndrome. GeneReviews(®). University of Washington, Seattle (WA). Seattle Copyright © 1993–2025, University of Washington, Seattle. GeneReviews is a registered trademark of the University of Washington, Seattle. All rights reserved.

Mahmoud S, Gharagozloo M, Simard C, Gris D, 2019. Astrocytes maintain glutamate homeostasis in the CNS by controlling the balance between glutamate uptake and release. Cells 8 (2).

Marks AR, 2023. Targeting ryanodine receptors to treat human diseases. J. Clin. Invest 133 (2).

McILwAIN H, 1969. In: Jasper HH, Ward AA (Eds.), Basic Mechanisms of the Epilepsies.

Mikati MA, Jiang YH, Carboni M, Shashi V, Petrovski S, Spillmann R, Milligan CJ, Li M, Grefe A, McConkie A, Berkovic S, Scheffer I, Mullen S, Bonner M, Petrou S, Goldstein D, 2015. Quinidine in the treatment of KCNT1-positive epilepsies. Ann. Neurol 78 (6), 995–999. [PubMed: 26369628]

Perea G, Araque A, 2005. Glial calcium signaling and neuron-glia communication. Cell Calcium 38 (3–4), 375–382. [PubMed: 16105683]

Pyott SJ, Duncan RK, 2016. BK channels in the vertebrate inner ear. Int. Rev. Neurobiol 128, 369–399. [PubMed: 27238269]

Rana PS, Gibbons BA, Vereninov AA, Yurinskaya VE, Clements RJ, Model TA, Model MA, 2019. Calibration and characterization of intracellular Asante potassium green probes, APG-2 and APG-4. Anal. Biochem 567, 8–13. [PubMed: 30503709]

Roy B, Han J, Hope KA, Peters TL, Palmer G, Reiter LT, 2020. An unbiased drug screen for seizure suppressors in duplication 15q syndrome reveals 5-HT(1A) and dopamine pathway activation as potential therapies. Biol. Psychiatry 88 (9), 698–709. [PubMed: 32507391]

Rulifson EJ, Kim SK, Nusse R, 2002. Ablation of insulin-producing neurons in flies: growth and diabetic phenotypes. Science 296 (5570), 1118–1120. [PubMed: 12004130]

Scharfman HE, 2007. The neurobiology of epilepsy. Curr. Neurol. Neurosci. Rep 7 (4), 348–354. [PubMed: 17618543]

Schauwecker PE, 2012. The effects of glycemic control on seizures and seizure-induced excitotoxic cell death. BMC Neurosci. 13, 94. [PubMed: 22867059]

Schröder W, Hinterkeuser S, Seifert G, Schramm J, Jabs R, Wilkin GP, Steinhäuser C, 2000. Functional and molecular properties of human astrocytes in acute hippocampal slices obtained from patients with temporal lobe epilepsy. Epilepsia 41 (Suppl. 6), S181–S184. [PubMed: 10999541]

Schwechter EM, Velísková J, Velísek L, 2003. Correlation between extracellular glucose and seizure susceptibility in adult rats. Ann. Neurol 53 (1), 91–101. [PubMed: 12509852]

Seifert G, Steinhäuser C, 2013. Neuron-astrocyte signaling and epilepsy. Exp. Neurol 244, 4–10. [PubMed: 21925173]

Sofroniew MV, Vinters HV, 2010. Astrocytes: biology and pathology. Acta Neuropathol. 119 (1), 7–35. [PubMed: 20012068]

Stafstrom CE, 2003. Hyperglycemia lowers seizure threshold. Epilep. Curr 3 (4), 148–149.

Staricha K, Meyers N, Garvin J, Liu Q, Rarick K, Harder D, Cohen S, 2020. Effect of high glucose condition on glucose metabolism in primary astrocytes. Brain Res. 1732, 146702. [PubMed: 32032612]

Stone B, Burke B, Pathakamuri J, Coleman J, Kuebler D, 2014. A low-cost method for analyzing seizure-like activity and movement in Drosophila. J. Vis. Exp 84, e51460.

Stork T, Bernardos R, Freeman MR, 2012. Analysis of glial cell development and function in Drosophila. Cold Spring Harb Protoc 2012 (1), 1–17. [PubMed: 22194269]

Walch E, Murphy TR, Cuvelier N, Aldoghmi M, Morozova C, Donohue J, Young G, Samant A, Garcia S, Alvarez C, Bilas A, Davila D, Binder DK, Fiacco TA, 2020. Astrocyte-selective volume increase in elevated extracellular potassium conditions is mediated by the Na(+)/K(+) ATPase and occurs independently of aquaporin 4. ASN Neuro 12, 1759091420967152.

Walz W, 2000. Role of astrocytes in the clearance of excess extracellular potassium. Neurochem. Int 36 (4–5), 291–300. [PubMed: 10732996]

Yamasaki K, Joh K, Ohta T, Masuzaki H, Ishimaru T, Mukai T, Niikawa N, Ogawa M, Wagstaff J, Kishino T, 2003. Neurons but not glial cells show reciprocal imprinting of sense and antisense transcripts of Ube3a. Hum. Mol. Genet 12 (8), 837–847. [PubMed: 12668607]

Zheng N, Shabek N, 2017. Ubiquitin ligases: structure, function, and regulation. Annu. Rev. Biochem 86, 129–157. [PubMed: 28375744]

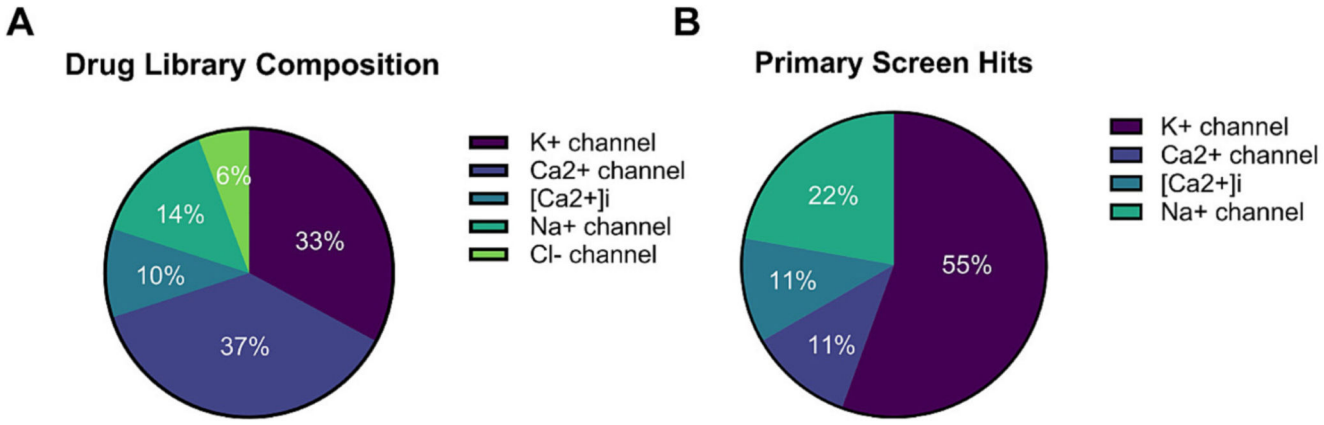

Fig. 1.

Primary screening identifies K^+ agonists as a likely mechanism of seizure suppression in *repo* > *Dube3a* flies. A) Pie chart illustrating the distribution of physiological targets for all 70 compounds in the Enzo SCREEN-WELL Ion Channel Library. 33 % target K^+ channels, 37 % target Ca^{2+} channels, 10 % target intracellular Ca^{2+} channels, 14 % target Na^+ channels, and 6 % target Cl^- channels. B) Pie chart showing the breakdown of physiological targets for the 12 compounds that successfully passed the primary drug screen. Notably, 55 % of these compounds target K^+ channels.

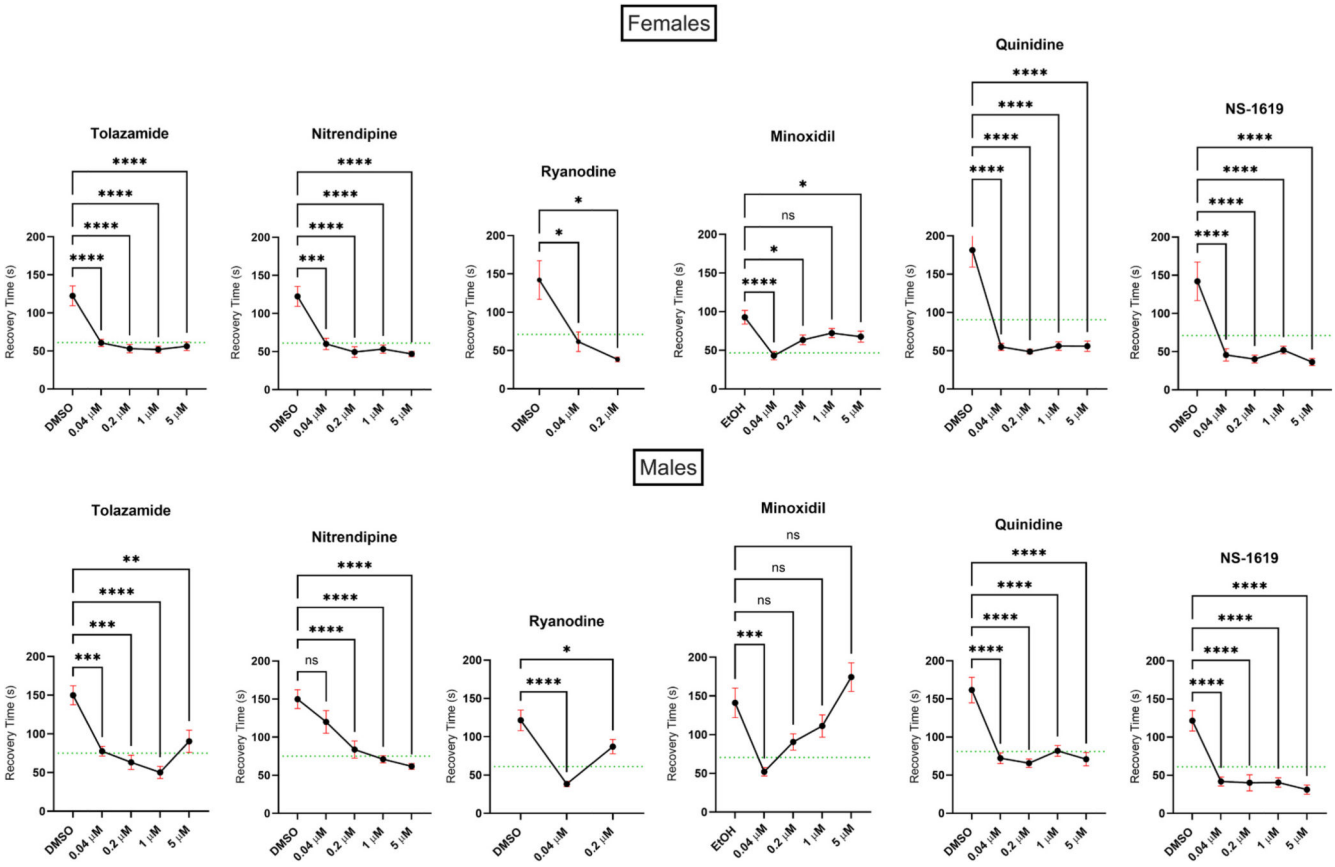

Fig. 2.

Secondary screen reveals six compounds that significantly reduce seizure duration in *repo* > *Dube3a* flies. Mean recovery times for male and female *repo* > *Dube3a* flies raised on either control food (solvent only) or drug food. The green line represents a 50 % reduction in recovery time compared to the control. Of the 11 compounds evaluated during secondary screening, six were able to improve recovery time by 50 % in both males and females. Analysis by one-way ANOVA $p_{value} \leq 0.05$ for significance. Error bars are mean ± SEM.

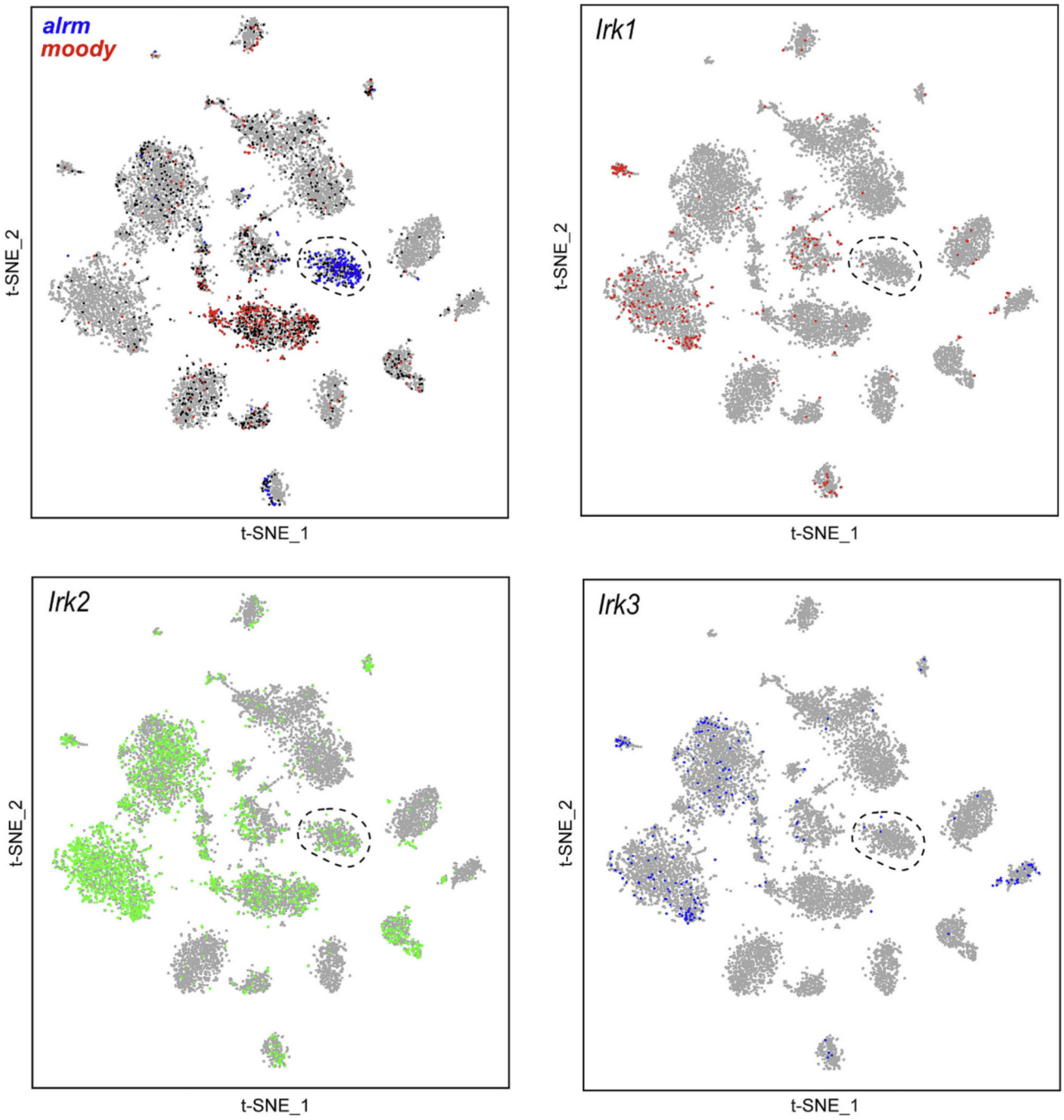

Fig. 3.

Glial scRNA-seq analysis reveals the expression of *Irk2* primarily in Drosophila astrocytes. *In silico* glial scRNA-seq analysis in Drosophila, visualized using t-distributed stochastic neighbor embedding (t-SNE), reveals distinct clustering of glial subtypes. The green clusters correspond to *nrv2*-positive ensheathing, subperineurial, cortex, and astrocytic glia. The red cluster represents *moody*-positive subperineurial glia, while the blue cluster identifies *alrm*-positive astrocytes. Co-expression analysis of *Irk1*, *Irk2*, and *Irk3* reveals that *Irk2* is exclusively expressed in *alrm*-positive astrocytes. (scope.aertslab.org).

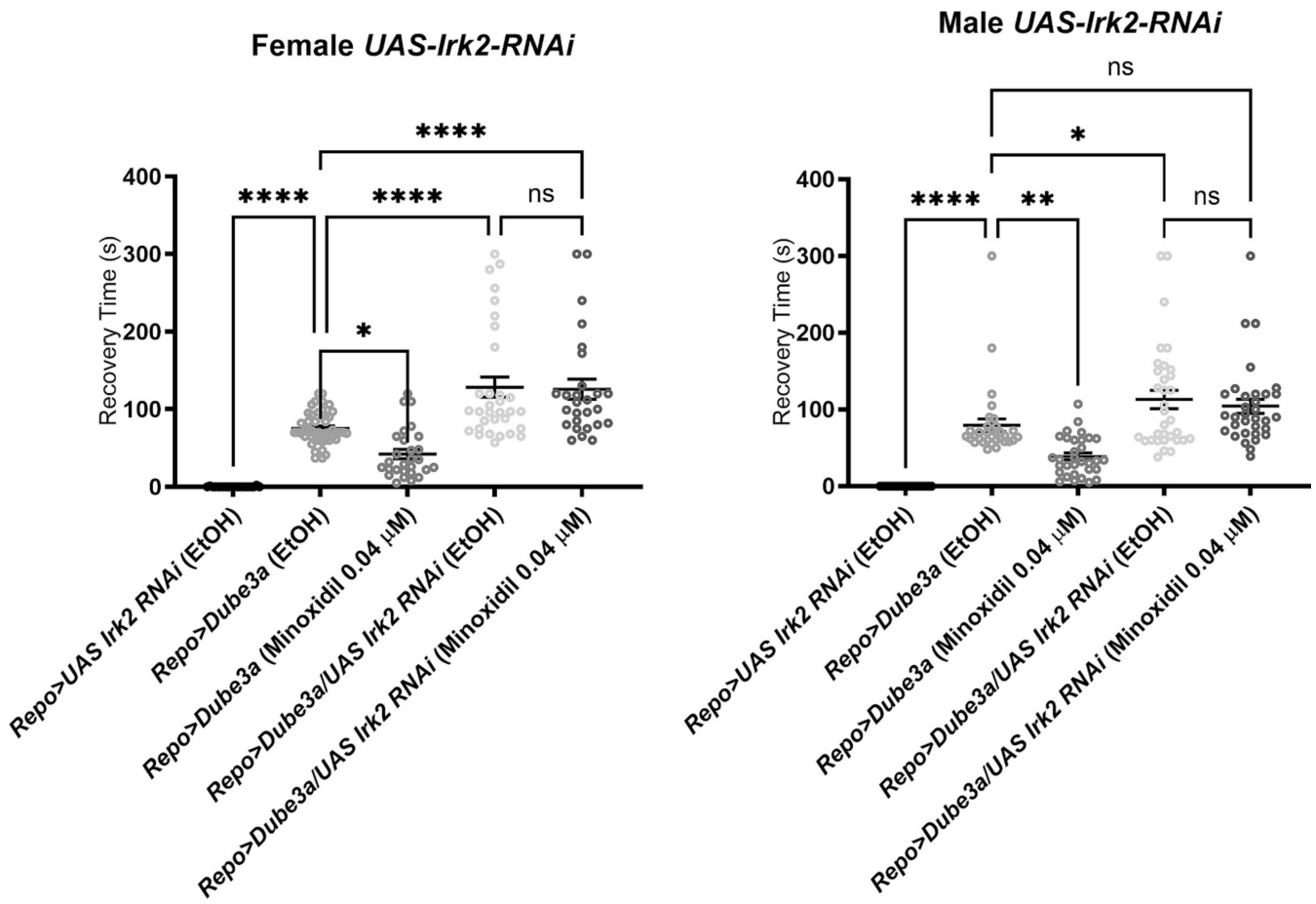

Fig. 4.

Seizures in *Irk2* glial-specific KD animals are not rescued by minoxidil. Seizure recovery times were analyzed in both male and female flies across the following genotypes and treatments: *repo* > *Irk2-RNAi/+*, *repo* > *Dube3a/+*, *repo* > *Dube3a* treated with 0.04 μM minoxidil, *repo* > *Dube3a/Irk2-RNAi*, and *repo* > *Dube3a/Irk2-RNAi* treated with 0.04 μM minoxidil. In both sexes, *repo* > *Dube3a/Irk2-RNAi* flies displayed significantly longer recovery times compared to *repo* > *Dube3a/+* flies. While the addition of minoxidil had no significant effect on recovery times in males with the *repo* > *Dube3a/Irk2-RNAi* genotype, it significantly increased recovery times in females compared to *repo* > *Dube3a/+*. Analysis by one-way ANOVA $p_{value} \leq 0.05$ for significance. Error bars are mean ± SEM.

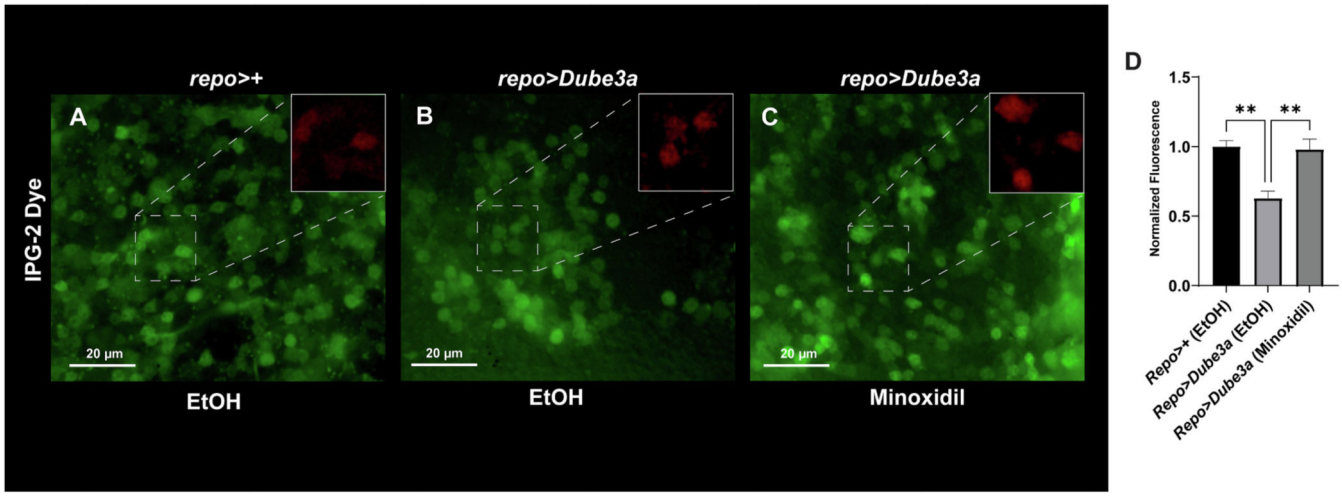

Fig. 5.

Minoxidil treatment of *repo > Dube3a* flies rescues glial intracellular K^+ content. Drosophila brains incubated in IPG-2 K^+ sensing dye (ION Biosciences). A) Representative image of *repo > tdTomato* show basal $[K^+]_i$ in the Drosophila brain. B) Representative image of *repo > Dube3a; tdTomato* treated with EtOH show a net decrease in $[K^+]_i$. C) Representative image of *repo > Dube3a; tdTomato* treated with 0.04 µM minoxidil show rescue of the $[K^+]_i$. D) Normalized fluorescent quantification for 60× images (A-C). IPG-2 quantification displays a significant rescue of $[K+]_i$ in glia for *repo > Dube3a; tdTomato* treated with minoxidil. Zoomed in panels represent an example of corresponding IPG-2 quantified *repo > Dube3a; TdTomato* positive cells. For each condition, a minimum of six flies were analyzed, with at least 120 cells examined per condition. Analysis by one-way ANOVA $p_{value} \leq 0.05$ for significance. Error bars are mean ± SEM.

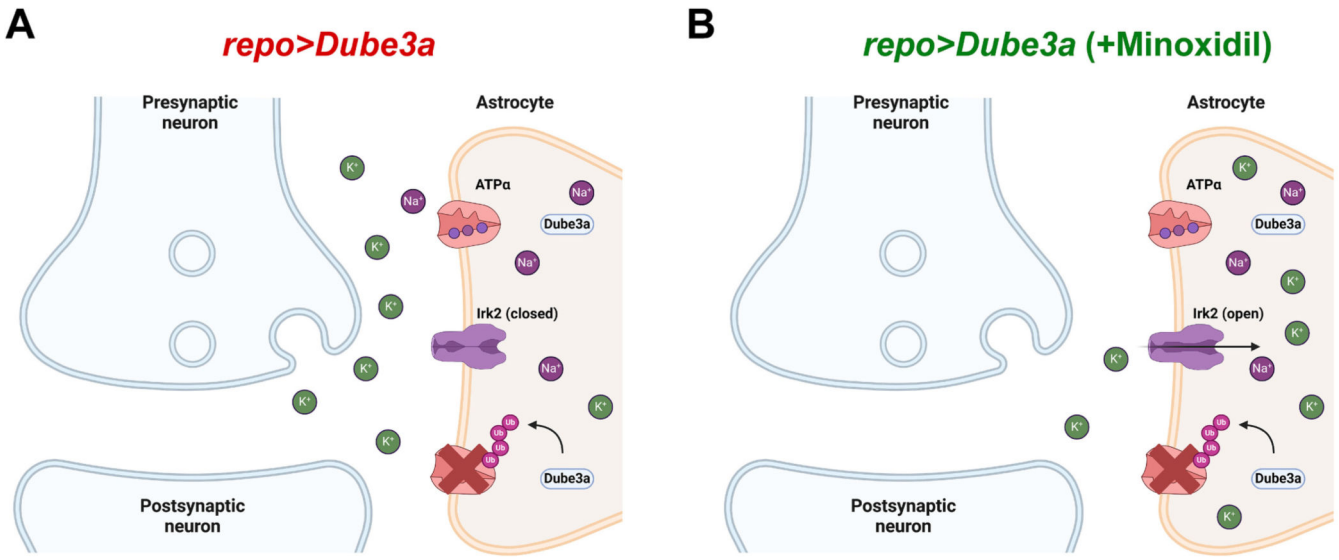

Fig. 6.

Proposed mechanism by which astrocytic Irk2 activation reduces neuronal excitability. A) In pathological conditions, *UBE3A* overexpression leads to the ubiquitin-mediated degradation of the Na^+/K^+ ATPase (ATPα), impairing astrocytic K^+ clearance, resulting in elevated extracellular potassium ($[K^+]_o$) levels, which contributes to neuronal hyperexcitability. B) Activation of astrocytic Irk2 channels, through agonists like minoxidil, promotes K^+ influx into astrocytes, counter-balancing elevated $[K^+]_o$ and reducing the likelihood of unwanted action potentials.

Table 1

Percent suppression is the percentage of flies expressing *Dube3a* in glia that were not seizing post-vortexing.

	Seizure		No Seizure			
Compound	***repo* > *Dube3a***	**UAS-*Dube3a*; TM3, *Sb***	***repo* > *Dube3a***	**UAS-*Dube3a*; TM3, *Sb***	**Total # *repo* > *Dube3a***	**Percent Suppression**
DMSO	16	0	0	92	16	0
Water	23	1	1	154	24	4
Diazoxide	5	0	8	56	13	61
E-4031•2HCl • 2H2O	2	0	5	60	7	71
FPL-64176	9	2	16	80	25	64
Gingerol	7	0	27	124	34	79
Minoxidil	1	1	4	78	5	80
Nitrendipine	3	1	4	48	7	57
NS-1619	3	3	9	83	12	75
Paxilline	10	0	18	92	28	64
Quinidine·HCl·H2O	1	0	5	71	6	83
Ryanodine	2	5	2	69	4	50
Tolazamide	5	0	11	78	16	68